Preprint from:

OPERA IPOGEA

Journal of Speleology in Artificial Cavities

Special Issue 2020

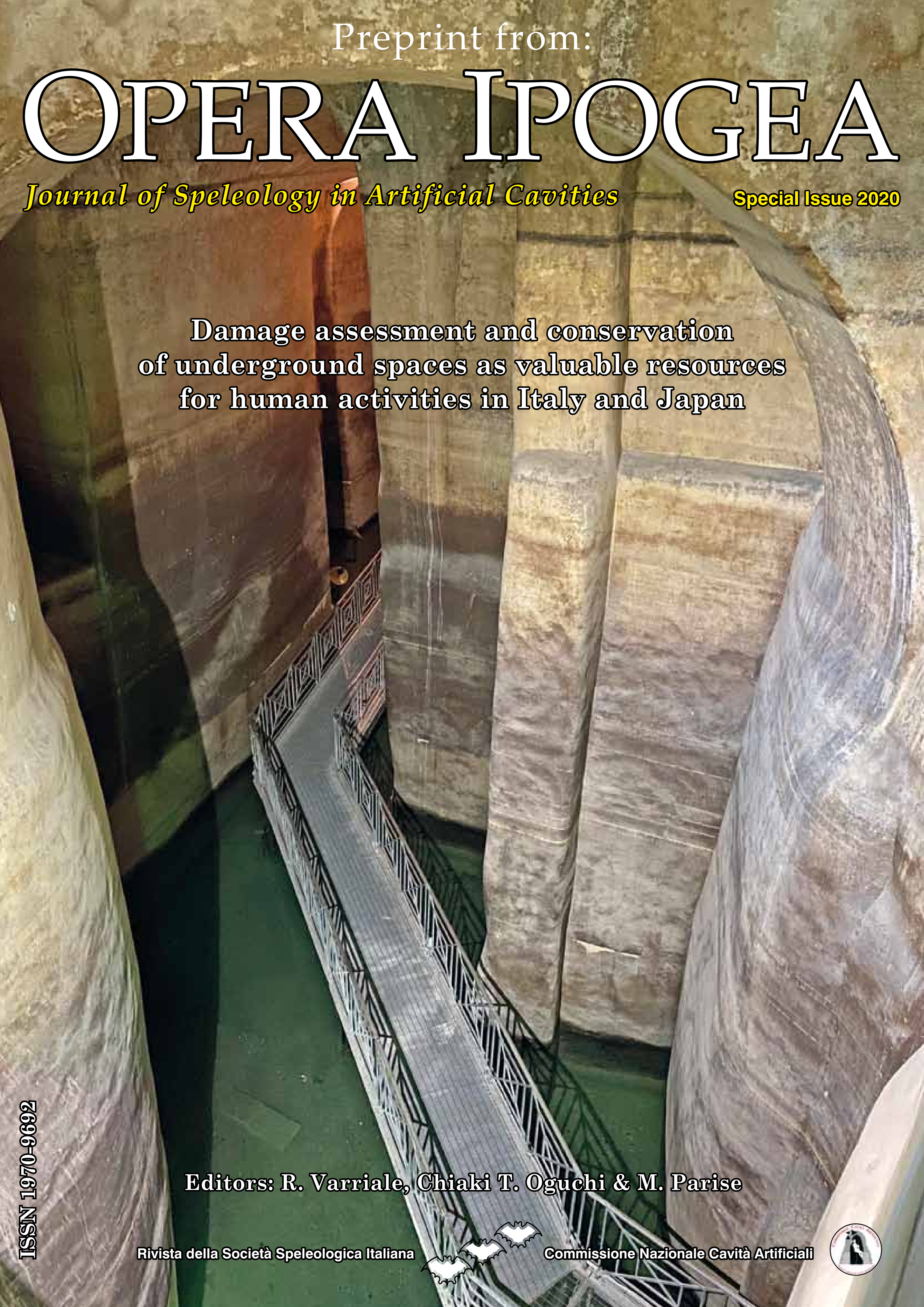

Damage assessment and conservation of underground spaces as valuable resources for human activities in Italy and Japan

Editors: R. Varriale, Chiaki T. Oguchi & M. Parise

ISSN 1970-9692

Rivista della Società Speleologica Italiana

Commissione Nazionale Cavità Artificiali

Indice

Indice

Indice

OPERA IPOGEA

Memorie della Commissione Nazionale Cavità Artificiali
www.operaipogea.it

Semestrale della Società Speleologica Italiana
Semi-annual of the Italian Speleological Society

Anno / *Year 22* – Numero Speciale / *Special Issue 2020*
Autorizzazione del Tribunale di Bologna n. 7702 dell’11 ottobre 2006
Authorization of the Court of Bologna n. 7702 of 11th October 2006

Proprietario / *Owner*
Società Speleologica Italiana

Sede della Redazione / *Editorial office*
c/o Andrea De Pascale - Corso Magenta, 29/2 - 16125 Genova, Italia
andreadepascale@libero.it

Composizione e impaginazione / *Composition and layout*
Fausto Bianchi, Enrico Maria Sacchi

Copertina / *Cover*
Cisterna il Palombaro Lungo a Matera, Basilicata, Italia (foto: Archivio Antros – Matera)
Palombaro Lungo water tank in Matera, Basilicata, Italy (photo: Antros Archive – Matera)

Quarta di copertina / *Back cover*
Chiesa K4c a Göreme, Cappadocia, Turchia (foto: Archivio Centro Studi Sotterranei – Genova)
K4c church in Göreme, Cappadocia, Turkey (photo: Centre for Underground Study Archive – Genoa)

Prezzo di copertina / *Cover price*
Euro 25,00

Tipografia / *Print*
A.G.E. s.r.l. – Via della Stazione, 41 - 61029 Urbino (PU) - Italia - Tel. +39 0722 328756

Monitoring UBH: detecting the main structural features and tracking them along acquisitions (temporally spaced) in order to prevent collapses or to understand pressure and movements in progress

Monitoraggio del patrimonio culturale sotterraneo: identificazione di elementi strutturali al fine della prevenzione di crolli o per la valutazione di movimenti

Marco Leo[1], Arturo Argentieri[1], Pierluigi Carcagnì[1], Paolo Spagnolo[1], Pier Luigi Mazzeo[1], Cosimo Distante[1]

Abstract

This paper summarizes the study, implementation and test phases of an algorithmic pipeline aiming at monitoring change on surfaces by using a low-cost optical device. The proposed algorithmic pipeline works on data acquired from a low-cost LIDAR and consists of different steps that aim at improving data also by exploiting very recent technologies based on convolutional neural networks.The improved data are then used to monitor changes in Underground Built Heritage (UBH). The high accuracy in terms of the minimum size of detectable changes has been quantified by experiments in the laboratory. Then, qualitative proofs of usage are reported by considering two case studies: the cave under Villa Pavoncelli in Naples and Taya Cave in Japan.

Keywords: Terrestrial Laser Scanner, deep learning super-resolution techniques, Iterative Closest Point, Point Feature Histograms, bilateral filter.

Riassunto

In questo articolo sono riportati i fondamenti teorici, i dettagli implementativi e i risultati sul campo di un nuovo sistema di monitoraggio delle superfici. In particolare il sistema è stato studiato, progettato e testato per la rilevazione di cambiamenti nelle superfici di aree di patrimonio costruito nel sottosuolo. Il sistema proposto è costituito da un sensore ottico a basso costo e da una serie di moduli software che, sfruttando recenti metodologie di apprendimento profondo, permettono di migliorare l'affidabilità e la precisione dei dati acquisiti dal sensore. I contributi di questo documento sono duplici. Da un lato, un LIDAR a basso costo è stato personalizzato al fine di svolgere l'attività richiesta in modo sicuro e coerente con l'obiettivo finale, che è quello di monitorare continuamente il patrimonio ipogeo costruito dall'uomo al fine di prevedere in anticipo eventi catastrofici come i crolli. Questa fase critica della progettazione e implementazione del dispositivo di acquisizione è riportata nella prima delle due sottosezioni seguenti. D'altro canto, i dati acquisiti devono essere elaborati per essere conformi all'accuratezza richiesta nel campo di applicazione considerato. La pipeline algoritmica esegue l'allineamento, il sovra-campionamento, la pulizia e il confronto dei dati. Nell'articolo si rendicontano le tre fasi della sperimentazione effettuate rispettivamente nel laboratorio di visione artificiale presso l'Istituto di Scienze Applicate e Sistemi Intelligenti del Consiglio Nazionale delle Ricerche d'Italia (CNR) a Lecce, nel caso di studio delle grotte di Villa Pavoncelli a Napoli (Italia) e nel caso di studio della Taya Cave in Giappone.

Parole chiave: Laser Scanner terrestre, tecniche di approfondimento profondo, Iterative Closest Point, filtro bilaterale.

[1] Institute of Applied Sciences and Intelligent Systems (ISASI), National Research Council of Italy (CNR), Lecce, Italy
Corresponding author: Marco Leo – marco.leo@cnr.it

Introduction

Three-dimensional laser scanning, also known as Light Detection and Ranging (LIDAR) or Terrestrial Laser Scanner (TLS), has quickly been expanding in recent years its applications for remote sensing in different research fields such as robotics (Suger *et al.*, 2015), agriculture (Weiss & Biber, 2011), transportation (Williams *et al.*, 2013), earth and ecological sciences (Eitel *et al.*, 2016).

In particular LIDAR technology has been exploited in the field of engineering geology, due to its ability to rapidly acquire highly accurate 3D positional data. If scans are taken multiple times in the same environment, LIDAR scanning can be applied to monitor and measure changes and deformations, as recently demonstrated in many studies dealing with engineering geology and slope stability (Jaboyedoff *et al.*, 2007, 2012; Brodu & Lague, 2012; Delaloye *et al.*, 2012; Lato *et al.*, 2013; Fazio *et al.*, 2017).

Previous work has demonstrated the feasibility of detecting changes based on comparisons of LIDAR scans captured before and after deformation has occurred. The simplest method for detecting deformation is to compute the distance between the nearest corresponding points in each scan (Zhizhong & Lu, 2011). Another approach is the use of minimum-distance projection to compare subsequent scan data and determine local deformations (Han *et al.*, 2013). An improvement of the point-to-point method is to generate meshed surfaces from scan data and compute surface-to-surface distances to detect changes (Barnhart & Crosby, 2013). The main drawback of using LiDAR scanning for deformation monitoring is that the raw point accuracy is generally below the magnitude of the smallest level of deformations that need to be measured. To address this, denoising techniques for profile analysis are recommended in order to improve data accuracy (Han *et al.*, 2017). The repeated application of terrestrial laser scanner to the same area (i.e., multi-temporality) allows increasingly improve accuracy (Abellan *et al.*, 2016; Dewez *et al.*, 2016). These approaches rely on the comparison of Digital Elevation Models (DEMs) to produce a new DEM called "DEM of Differences" (DoD) (Bossi *et al.*, 2015) but, unfortunately, they cannot operate properly on complex 3D environments since DEMs require a plane of reference (typically on the XY coordinates plane), and thus have issues when dealing with rough surfaces (Esposito *et al.*, 2017).

Furthermore, the most accurate laser scanners are very expensive (even more than 120,000$) and therefore out of reach for non-professional-users. On the other hand, in critical situations, it is necessary to continuously monitor the state of the underground natural structures. As mentioned above, it is unreasonable to leave an expensive tool permanently active, which moreover requires technical knowledge to be correctly used.

Fortunately, thanks to the rapid development of data processing and representation methods, there is a way to get around the aforementioned issues.

This paper proposes a pioneering study aiming at demonstrating how a proper algorithmic pipeline can, starting from scattered and noisy data extracted from a low-cost sensor, allows to extract very precise and accurate metrology information that can be used for monitoring Underground Built Heritage (UBH) sites.

The proposed approach works on data acquired from a low-cost LIDAR and consists of different steps that aim at improving data also by exploiting very recent technologies based on convolutional neural networks.

The following sections introduce the details of the proposed approach and reports on the experimentation carried out in the computer vision lab at the Institute of Applied Sciences and Intelligent Systems of the National Research Council of Italy (CNR) in Lecce and in the selected case studies, namely the caves of Villa Pavoncelli in Naples (Italy) and Taya Cave in Japan.

The proposed solution

The contributions of this paper are double fold. On the one side, a low-cost LIDAR has been customized in order to accomplish a safe and consistent continuous monitor of UBH sites in order to early predict catastrophic events like collapses. This critical phase of designing and implementing the acquisition device is reported in the first of the two following subsections.

On the other hand, acquired data have to be processed in order to be compliant with the accuracy required in the considered application field. The algorithmic pipeline performing data alignment, upsampling, denoising, and comparison is described in the second of the following subsections.

Design and implementation of the acquisition device

The sensing device used in this paper is a Sweep Scanse v0.991. The device is an off-the-shelf product made available by Scanse (https://www.youtube.com/c/ScanseIos). Scanse Sweep is designed with a sensing technique that takes an edge over low-power components. This is a scanning LIDAR sensor designed to bring powerful 360-degree sensing capabilities to everyone for an affordable price. This device has a built-in LIDAR-Lite that allow you to tweak the rotation speed on the fly, so that it is either possible to quiet it down for a detailed-info, or rush it up for faster reaction times.

The device weights 120 g and measures 65 x 50.9 mm, it can sense within a range of 40 meters, a sample rate of 1000 samples/second, thus, making it perfect for site surveying, robotics, UAVs, and Internet of Things/security applications. The device holds a sensor module that is enclosed with a rotating head making it operated by a small drive motor for a 360-degree field of view.

Sweep is a single-plane scanner. In layman terms, as its head rotates counter-clockwise, it collects the information or data in a single plane. This device can

a) The LIDAR sensor   b) The 3D printed housing   c) The electronic prototyping platform

Fig. 1 – The hardware components of the system (photo: ISASI/CNR©).
Fig. 1 – I componenti hardware del sistema (foto: ISASI/CNR©).

be connected to all low-level micro-controllers directly using its serial port or to any device such as a PC with the provided USB-to-serial converter. The feature that makes Scanse Sweep standing out from others tools is that it has two serial port connectors with identical signals that enable more mounting options.
The CNR technicians printed a 3D housing of the device and implemented the interface for remote control via a open-source electronics prototyping platform. Through this system, a controlled one-degree rotation (stepper) functionality was achieved. The housing is compliant to allow the device to be mounted on a tripod. In figure 1 the main hard-components are represented.

Data acquisition and processing

The algorithmic pipeline is schematized in figure 2. Since the algorithmic pipeline relies on multiple ac-

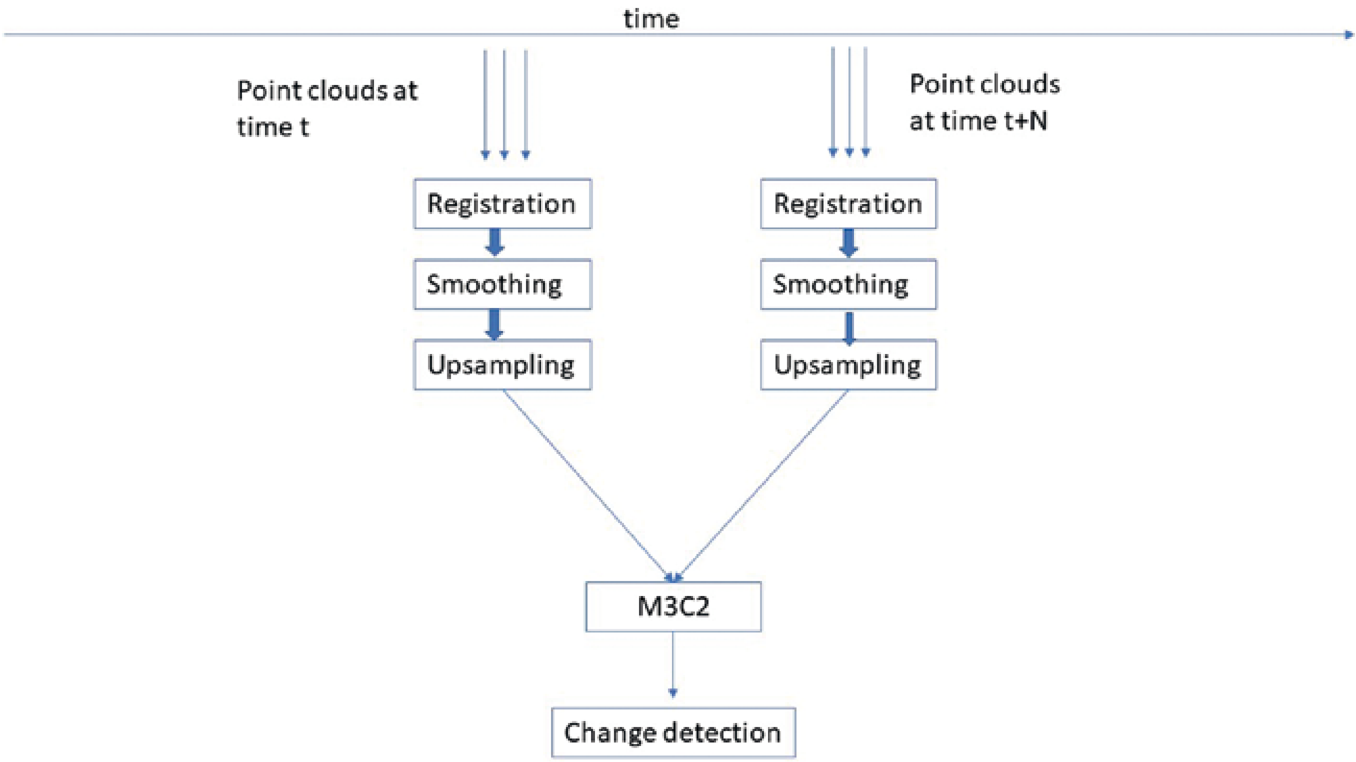

Fig. 2 – Scheme of the implemented pipeline (graphic: ISASI/CNR©).
Fig. 2 – Schema dei moduli software implementati e loro relazioni (grafica: ISASI/CNR©).

quisitions to increase pointwise accuracy, different overlapping 3D models need to be acquired during the same acquisition campaign. Acquisitions are stored on a laptop connected to the device by Wi-Fi technology. The first step in data processing concerns loading the scans. Successively, the overlapping areas among scans are used for alignment. The alignment task can be carried out with different approaches. It can be accomplished by matching targets captured in different scans, i.e. by using semantic features (e.g. objects) within the scans as reference points for alignment, or alternatively, in case of non-structured scenes (i.e. when scanning natural environments), computer-driven algorithms perform better since they make use of lower-level information than semantic features.

The most common computer-driven alignment is the Iterative Closest Point (ICP) algorithm which is a data-driven registration method. Traditional ICP algorithm registration is slow, especially when the scale of the point cloud is relatively large. In order to fix computational issues, recent alignment strategies rely on two sequential steps: first, a preliminary coarse registration, and then the classical ICP algorithm is used as fine registration to further improve the accuracy of the overall registration (Rusu *et al.*, 2009).

In this research activity, coarse registration was performed by Point Feature Histograms (PFH), the informative pose-invariant local features which represent the underlying surface model properties at a given point P. Their computation is based on the combination of certain geometrical relations between the p's nearest k neighbours. They incorporate 3D point coordinates, and estimate normal surface, but are extensible to the use of other properties such as curvature, 2nd order moment invariants, etc. The features computation leverages on an optimized algorithm namely Fast PHF (FPFH) having linear-complexity instead of quadratic one.

The FPFH feature is a 33-dimensional vector. We use RANSAC for global registration. In each RANSAC iteration, n random points are picked from the source point cloud. The corresponding points in the target point cloud are detected by querying the nearest neighbour in the 33-dimensional FPFH feature space. A pruning step takes fast pruning algorithms to quickly reject false matches early. Only matches that pass the pruning step are used to compute a transformation, which is validated on the entire point cloud. The maximum number of RANSAC iterations and the maximum number of validation steps are the two parameters to be set. For performance reasons, the global registration is only performed on a heavily down-sampled point cloud. The roughly aligned point clouds are then supplied to the ICP procedure to get a finer registration. The point-to-plane ICP algorithm is used because it has faster convergence speed than the point-to-point ICP algorithm.

After the alignment of the available overlapping point clouds, data filtering has to be performed. Point sets obtained by 3D scanners are often corrupted with noise that can have several causes, such as a tangential acquisition direction, changing environmental lights, or a reflective object material. It is thus crucial to design efficient tools to remove the noise from the acquired data, without removing important information such as sharp edges or shape details.

Filtering can be either user-driven or be completed using a filtering algorithm. User-driven filtering can be done to remove large anomalies in the scan, such as pieces of equipment or machinery. It is not practical to use user-driven filtration to remove smaller and near-surface anomalies, as it is too time-consuming. The bilateral filter for point cloud has been extensively used in noise reduction since 1998; it can be considered as a method that builds a filter kernel using guidance point cloud (Tomasi & Manduchi, 1998). The idea was to de-noise a pixel not only by considering the colour values of its Euclidean neighbours, but also the values of the neighbours that are close, both in position and in colour value. This concept was adapted to the denoising of meshes and can be extended to point clouds easily (Digne & De Franchis, 2017). The parameters for the bilateral filter are the following: the number of iterations N; the radius for the neighbourhood search r; the Gaussian weight for the Euclidean distance σ_d, and the Gaussian weight for the distance to the tangent plane σ_n.

The problem of setting the parameters can be simplified by considering that r and σ_d are related: the neighbours which are at distance farther than 3 σ_d barely contribute to the de-noising since their weight is almost 0. To avoid unnecessary computations, these points should simply be ignored. Therefore, one can set both parameters by choosing a radius r and setting $\sigma_d = (1/3)\ r$ and $\sigma_n = (1/3)\ r_n$, where r_n is the normal radius. In the experimental phase r = 0.05, r_n = 10 were used.

The smoothed point cloud is then given as input to a detail-driven deep neural network for point set upsampling.

Starting from the unordered set of 3D points, the network generates a denser point set that lies on the underlying surface. In the application context of monitoring UBH, this is a very challenging problem since the point set is relatively sparse and the underlying surface has complex geometric and topological structures.

The network configuration has been recently proposed (Yifan *et al.*, 2019) and it relies on an end-to-end progressive learning technique for point set upsampling. Intuitively, we train a multi-step patch-based network to learn the information from different levels of detail. More specifically, the approach consists of a sequence of upsampling network units. Each unit has the same structure, but we employ it on different levels of detail. The information of all levels is shared via our intra-level and inter-level connections inside and between the units. By progressively training all network units end-to-end, significant improvements in the point set are achieved.

Up sampled point cloud is then stored and it represents the reference model for the following acquisitions.

It is argued that this method produced fairly homogeneous data to be used in the point cloud comparison and analysis. This is done by a multi-temporal 3-D surveying data comparison based on Multiscale Model to Model Cloud Comparison (M3C2) (Lague *et al.*, 2013) that is of particular use in earth science because it incorporates a confidence interval and thus provides 3-D analysis of topographic change constrained by spatially variables and it is applicable in any type of surface. Within the M3C2 algorithm, measurement precision is estimated from local surface roughness, which is highly appropriate for the TLS data for which it was primarily designed.

The special case of RGB images

The proposed pipeline starts from point cloud data. Since it is possible that this kind of data is not available, a modification of it can exploited to analyze RGB image data. It is worth noting that only movements perpendicular to the optical axis can be detected but, in some cases, this can be enough for monitoring and preserving UHB.
In this case, image registration is performed by dense feature matching (Liu *et al.*, 2008), smoothing is still performed by bilateral filtering, upsampling is not necessary and finally, image comparison is again carried out exploiting structural features (Fazio *et al.*, 2019).

Experimental Results

To determine the accuracy of LiDAR in detecting scene changes, preliminary experiments have been carried out in the laboratory. The goal of this experimental phase is to determine in a systematic way the accuracy of the system. The experimental setup consists of different sized rectangular boxes. Boxes have been placed at different distances from the acquisition device, with distance ranging from 1 to 6 meters. The boxes were placed close to a wall of the laboratory, in such a way as to create discontinuous surfaces. Subsequently, only one box was moved (0.5 cm at a time), both along a direction parallel, and then perpendicular to the wall. Each time the box moved, at least 4 acquisition sessions were carried out.
Figure 3 shows the experimental setup in the laboratory (on the left) and the experimental outcomes (on the right). It demonstrates how the proposed pipeline reduces uncertainty in measurements. It also suggests to the system designers to introduce some way to make the device closer to the inspecting surface since, up to 3 meters of distance, the errors in measurements are very low whereas with large distances, the error, although lower than 5 cm, could affect the automatic process of detection in structural changes in a real case.

The case study in Italy

The implementing hardware and software solutions have been exploited to monitor underground quarry under the case-study of Villa Pavoncelli at Via Posillipo 26 in Naples, Italy.
The quarry environment is humid (there are sewage drains and the sea is just a few meters away), the sloping terrain is unstable because it consists of sand and stones, and for this reason, it is not suitable for fixed installations of technological instruments. The height of the quarry is about 5 meters at the highest point, with very irregular rock walls, and different areas with exposed roots from the overhanging trees. From the rock walls, failures often occur due to the weight of the overlying palace and the adjoining garden.
Figure 5 shows two pictures taken inside the quarry during a data acquisition campaign and 2 point clouds acquired using the device at a rotation frequency of 1 Hertz and a sampling rate of 1000 Hertz.

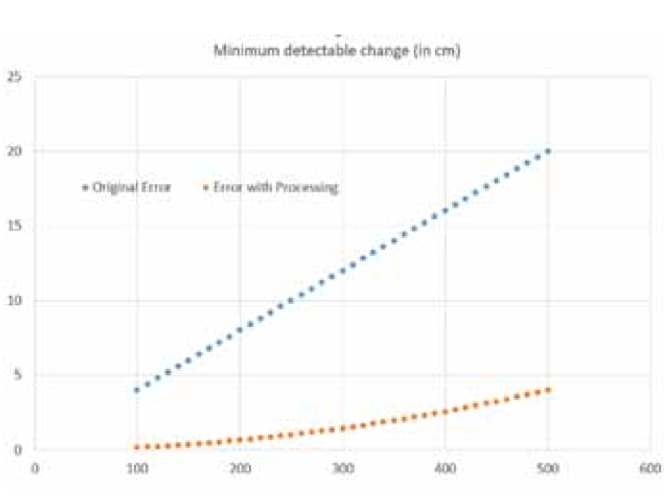

Fig. 3 – The experimental setup in the laboratory (on the left) and the experimental outcomes (on the right) (photo: ISASI/CNR©).
Fig. 3 – La configurazione sperimentale (a sinistra) ed i risultati ottenuti in laboratorio (foto: ISASI/CNR©).

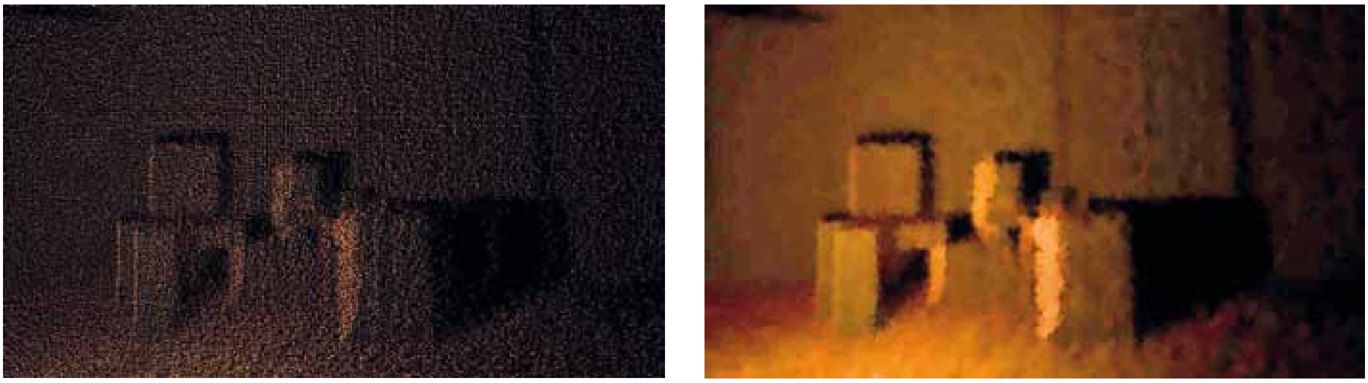

Fig. 4 – On the left, a rough point cloud acquired in the lab. On the right the effect of the processing n the same data set. Smoothing and up-sampling allow having more uniform objects' surfaces while preserving their borders (photo: ISASI/CNR©).

Fig. 4 – A sinistra, una nuvola di punti grezza acquisita in laboratorio. A destra l'effetto del trattamento nello stesso set di dati. La levigatura e il sovra-campionamento consentono di avere superfici di oggetti più uniformi preservandone i bordi (foto: ISASI/CNR©).

Fig. 5 – Two pictures of the quarry chosen as a case study (first row) and (below) two rough point clouds acquired in a preliminary acquisition campaign (photo: ISASI/CNR©).

Fig. 5 – Due immagini della cava scelta come caso di studio (in alto) e (in basso) due nuvole di punti grezze acquisite in una campagna di acquisizione preliminare (foto: ISASI/CNR©).

Fig. 6 – The results of the comparison between the acquisitions. Two screenshots of the same resulting point cloud are reported. No difference has been found in the surface area of the roof (photo: ISASI/CNR©).

Fig. 6 – I risultati del confronto tra le acquisizioni. Sono riportate due istantanee della stessa nuvola di punti risultante. Nessuna differenza è stata individuata nella superficie del tetto (foto: ISASI/CNR©).

To acquire the surface to be monitored and ensure adequate overlap between the different point clouds, 6 different points of the acquisition have been identified (i.e., points where to locate the device).
The six acquisition points extend over the ground in a row of two, from the highest to the lowest part. All the acquisitions have to be processed (aligned and filtered) in order to get a unique representation of the quarry at the moment of acquisition. This representation could be then compared with that obtained on a different day.
In figure 6 the comparison of two representations gathered on two consecutive days (October 22nd and 23rd, 2018) is reported. As expected, given the temporal proximity of the two acquisitions, no difference has been found in the surface area of the roof. Anyway, this can be considered a preliminary proof of the validity of the proposed approach.

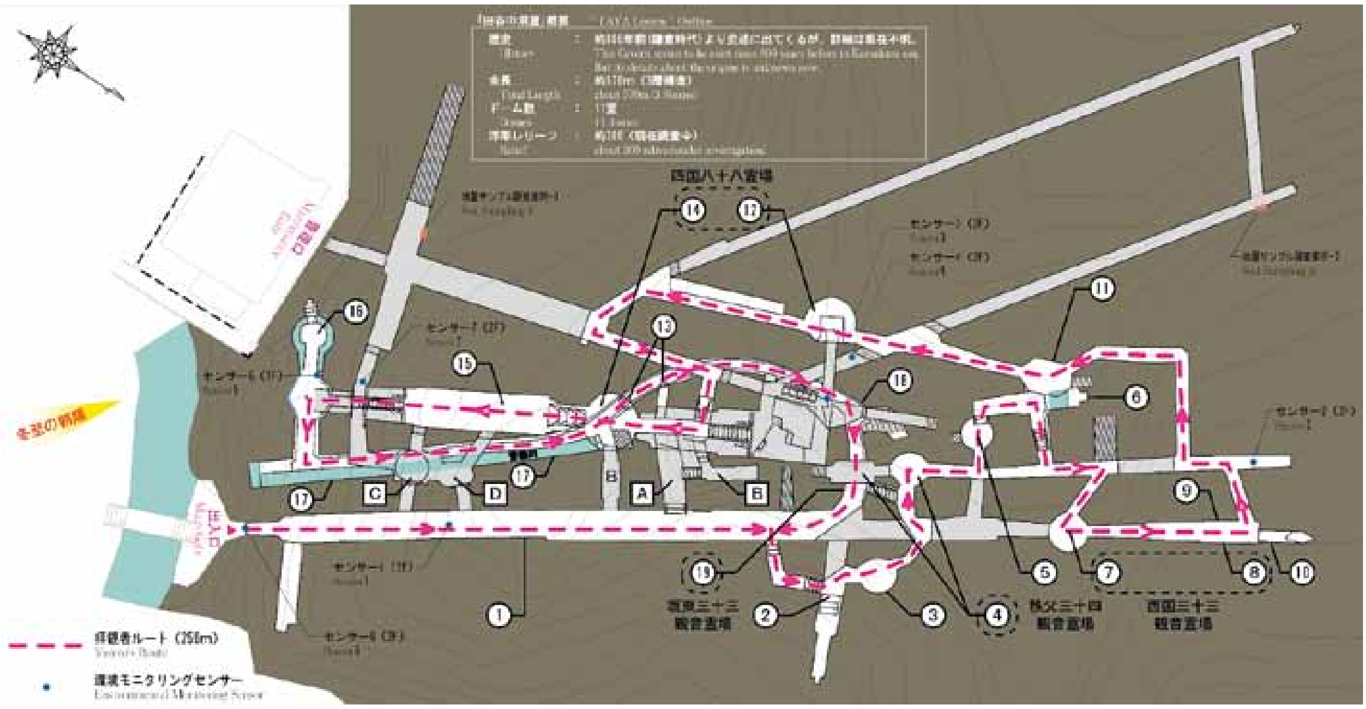

Fig. 7 – A map of the cave (ECPT © 2016-2019).

Fig. 7 – Mappa della grotta (ECPT © 2016-2019).

Fig. 8 – Some images acquired in the Taya Cave. From the images, it is possible to figure out that there is a very critical situation with structural failures in progress. Collapses can occur at any moment, putting visitors at risk (photo: ISASI/CNR©).

Fig. 8 – Alcune immagini acquisite nella grotta di Taya. Dalle immagini, è possibile capire che esiste una situazione molto critica con evidenti cedimenti strutturali in corso. I crolli possono verificarsi in qualsiasi momento, mettendo a rischio i visitatori (foto: ISASI/CNR©).

Fig. 9 – Result of two image matching. No differences have been found: as you can see detected feature points overlap (photo: ISASI/CNR©).

Fig. 9 – Risultato della corrispondenza tra due immagini. Non sono state rilevate differenze: come è possibile osservare, i punti di interesse rilevati si sovrappongono (foto: ISASI/CNR©).

Other acquisitions are planned in the next months in order to automatically point out changes in the quarry.

The case study in Japan

A slightly modified version of the pipeline has been also exploited to monitor a small portion of the Taya Cave, that is an artificial cave carved into a hillside on the outskirts of Kamakura by Shingon Buddhist monks from 1192 until 1720 (Jeremiah, 2006). It contains antique carvings of Buddhas, Buddhist saints, fantastic creatures, and Mantras carved in kanji and Sanskrit (the ancient Indian language in which the Buddhist sutras, or sacred texts) were originally written.
Taya Cave is a winding passageway more than 0.5 kilometer-long carved into an inconspicuous hillside behind the Jousenji temple. It is dimly lit along the way with weak LED bulbs.
For this case study, the input data were not 3D points but RGB images since it was not possible to move the 3D scan system to Japan.
In figure 7 a map of the cave is shown. The monitoring points are highlighted.
In figure 8 some images acquired in Taya Cave are reported. From the images, it is possible to figure out that there are many very critical situations with structural failures in progress. It is possible to observe that collapses can occur at any moment, putting visitors at risk. Finally, in figure 9 a preliminary result is reported: two images acquired in two consecutive days are compared and no differences have been found (as you can see detected feature points overlap).

References

Abellán A., Derron M.H., Jaboyedoff M., 2016, *'Use of 3D Point Clouds in Geohazards' Special Issue: Current Challenges and Future Trends*, Remote Sensing, 8, 130.

Barnhart T., Crosby B.T., 2013, *Comparing two methods of surface change detection on an evolving thermokarst using high-temporal-frequency terrestrial laser scanning, Selawik River, Alaska*, Remote Sensing, vol. 5 (6), pp. 2813-2837 DOI:10.3390/rs5062813.

Bossi G., Cavalli M., Crema S., Frigerio S., Quan Luna B., Mantovani M., Marcato G., Schenato L., Pasuto A., 2015, *Multi-temporal LiDAR-DTMs as a tool for modelling a complex landslide: a case study in the Rotolon catchment (eastern Italian Alps).* Natural Hazards and Earth System Sciences, vol. 15 (4), pp. 715-722 DOI: 10.5194/nhess-15-715-2015.

Brodu N., Lague D., 2012, *3D terrestrial lidar data classification of complex natural scenes using a multi-scale dimensionality criterion: applications in geomorphology*, ISPRS J Photogramm Remote Sensing, vol. 68, pp. 121-134.

Delaloye D., Hutchinson J., Diederichs M.A., 2012, *New Workflow For LiDAR Scanning For Change Detection In Tunnels and Caverns*, in: A. Bobet (ed.), Proc. US Rock Mechanics/Geomechanics Symposium. American Rock Mechanics Association, pp.1-8.

Dewez T.J.B., Girardeau-Montaut D., Allanic C., Rohmer J.F., 2016, *A CloudCompare plugin to extract geological planes from unstructured 3D point clouds*, ISPRS Int. Arch. Photogramm. Remote Sens. Spat. Inf. Sci., XLI-B5, pp. 799-804.

Digne J., De Franchis C., 2017, *The Bilateral Filter for Point Clouds*. Image Processing On Line, vol. 7, pp. 278-287. DOI: 10.5201/ipol.2017.179.

Eitel J., Hofle B., Vierling L.A., Abellan A., Asner G.P., Deems J.S., Glennie C.L., Joerg P.C., Lewinter A.L., Magney T.S., Mandlburger G., Morton D.C., Muller J., Vierling K.T., 2016, *Beyond 3-D: The new spectrum of lidar applications for earth and ecological sciences*, Remote Sensing of Environment, vol. 186, pp. 372-392.

Esposito G., Salvini R., Matano F., Sacchi M., Danzi M., Somma R., Troise C., 2017, *Multitemporal monitoring of a coastal landslide through SfM-derived point cloud comparison*, Photogramm. Rec., vol. 32 (160), pp. 459-479, DOI: doi.org/10.1111/phor.12218.

Fazio N.L., Perrotti M., Lollino P., Parise M., Vattano M., Madonia G., Di Maggio C., 2017, *A three-dimensional back analysis of the collapse of an underground cavity in soft rocks*, Engineering Geology, vol. 238, pp. 301-311.

Fazio N.L., Leo M., Perrotti M., Lollino P., 2019, *Analysis of the Displacement Field of Soft Rock Samples During UCS Tests by Means of a Computer Vision Technique*. Rock Mechanics and Rock Engineering, 1-18.

Han J.Y., Guo J., Jiang Y.-S., 2013, *Monitoring tunnel profile by means of multi-epoch dispersed 3-D LiDAR point clouds*, Tunnelling and Underground Space Technology, vol. 33, pp. 186-192 DOI: 10.1016/j.tust.2012.08.008.

Han X.F., Jin J.S., Wang M.J., Jiang W., Gao L., Xiao L., 2017, *A review of algorithms for filtering the 3D point cloud,* Signal Processing: Image Communication, vol. 57, pp. 103-112, DOI: 57. 10.1016/j.image.2017.05.009.

Jaboyedoff M., Metzger R., Oppikofer T., Couture R., Derron M., Locat J., Turmel D., 2007, *New insight techniques to analyze rock-slope relief using DEM and 3D-imaging cloud points: COLTOP-3D software*, Proc 1st Canada–US Rock Mech Symp, Vancouver, Canada.

Jaboyedoff M., Oppikofer T., Abellán A., Derron M.H., Loye A., Metzger R., Pedrazzini A., 2012, *Use of LIDAR in landslide investigations: a review*, Natural Hazards, vol. 61, pp. 5-28.

Jeremiah K., 2006, *Taya cave*. Kansai Time Out, vol. 352, pp. 35.

Lague D., Brodu N., Leroux J., 2013, *Accurate 3D comparison of complex topography with terrestrial laser scanner: Application to the Rangitikei canyon (NZ)*. ISPRS Journal of Photogrammetry and Remote Sensing, vol. 82, pp. 10-26.

Lato M., Kemeny J., Harrap R.M., Bevan G., 2013, *Rock bench: Establishing a common repository and standards for assessing rockmass characteristics using LIDAR and photogrammetry*, Computers & Geosciences, vol. 50, pp. 106-114.

Liu C., Yuen J., Torralba A., Sivic J., Freeman W.T., 2008, *Sift flow: Dense correspondence across different scenes*, in European conference on computer vision, Springer, Berlin, Heidelberg, pp. 28-42.

Rusu R.B., Blodow N., Beetz M., 2009, *Fast point feature histograms (FPFH) for 3D registration*, in the proc. of the 2009 IEEE International Conference on Robotics and Automation. (Kobe, 2009), pp. 3212-3217.

Suger B., Steder B., BurgardW., 2015, *Traversability analysis for mobile robots in outdoor environments: a semi-supervised learning approach based on 3D-lidar data*. Proc. 2015 IEEE International Conference on Robotics and Automation (ICRA), pp. 3941-3946.

Tomasi C., Manduchi R., 1998, *Bilateral filtering for gray and color images*, in Proc. of the Sixth International Conference on Computer Vision, (Bombay, India), pp. 839-846, DOI: 10.1109/ICCV.1998.710815.

Weiss U., Biber P., 2011, *Plant detection and mapping for agricultural robots using a 3D LIDAR sensor,* Robotics and autonomous systems, vol. 59 (5), pp. 265-273.

Williams K., Olsen M. J., Roe G.V., Glennie C., 2013, *Synthesis of transportation applications of mobile LiDAR*. Remote Sensing, vol. 5 (9), pp. 4652-4692.

Yifan W., Wu S., Huang H., Cohen-Or D., Sorkine-Hornung O., 2019, *Patch-based Progressive 3D Point Set Upsampling,* in: Proceedings of the IEEE Conference on Computer Vision and Pattern Recognition, pp. 5958-5967.

Zhizhong K., Lu Z., 2011, *The change detection of building models using epochs of terrestrial point clouds*, Proc. of the International Workshop on Multi-Platform/Multi-Sensor Remote Sensing and Mapping. M2RSM 2011, Xiamen, pp. 1-6 DOI: 10.1109/M2RSM.2011.5697381.